Available online at www.sciencedirect.com
SCIENCE DIRECT®
ELSEVIER
Journal of Nuclear Materials 329–333 (2004) 1066–1071
journal of nuclear materials
www.elsevier.com/locate/jnucmat

In-beam fatigue behavior of F82H steel at 500 °C

Y. Murase [a,*], Johsei Nagakawa [a,b], K. Chuto [a], N. Yamamoto [a]

[a] *Materials Engineering Laboratory, Materials Reliability Group, National Institute for Materials Science (NIMS), 1-2-1 Sengen, Tsukuba, Ibaraki 305-0047, Japan*

[b] *Interdisciplinary Graduate School of Engineering Sciences, Kyushu University, 6-1 Kasuga Koen, Kasuga, Fukuoka 816-8580, Japan*

Abstract

Stress-controlled fatigue tests were conducted for side-notched small specimens of F82H steel under in-beam and unirradiated conditions with 17 MeV protons at 500 °C. The environment for the fatigue tests was impure He gas containing 10–3000 ppm oxygen. The number of cycles to fracture (N_f) was slightly reduced under irradiation. SEM examination of fracture surfaces indicated the formation of an oxide film in the vicinity of notch tip only for the in-beam specimens. Optical microscopic observation demonstrated oxidation not only along the grain boundaries but also on the crystallographic slip planes on the specimen surfaces of both in-beam and unirradiated specimens. The oxidation appeared to be enhanced to form numerous oxidation pits on the surface, especially for the in-beam specimens. In this study, the in-beam fatigue behavior at 500 °C is discussed with respect to the dynamic irradiation effect in the low oxygen potential atmosphere.

1. Introduction

The low activation ferritic/martensitic steel F82H is one of the most promising candidates for the first wall and blanket materials of Tokamak-type thermonuclear fusion reactors. Since the cyclic operation of a fusion reactor gives rise to the combined loading of cyclic thermal and magnetic stresses and severe irradiation damage to fusion reactor materials, the understanding of fatigue behavior under irradiation is an important concern for fusion applications. Although several papers [1–4] have dealt with the in-beam fatigue behavior for some structural materials, more extensive accumulation of experimental data is definitely needed under well-designed parametric variations of experimental conditions. Murase et al. [5] have recently conducted stress controlled fatigue tests for F82H steel under 17 MeV proton irradiation at 60 °C. A substantial increase of fatigue life under irradiation has indicated the existence of a dynamic irradiation effect on fatigue behavior at 60 °C. In the present paper, the dynamic irradiation effect at 60 °C is designated as the lower temperature type (LT-type) dynamic irradiation effect. The mechanism of the LT-type dynamic irradiation effect can be explained in terms of the interaction between radiation-induced defect (RID) clusters and moving dislocations [5].

In the present study, stress-controlled tension–tension fatigue tests were performed for side-notched small specimens of F82H steel under irradiation and unirradiated conditions with 17 MeV protons at 500 °C. The environment was the impure He gas containing 10–3000 ppm oxygen. After the fatigue tests, the fracture surfaces of all specimens were examined by a scanning electron microscope (SEM). Optical microscopic observation of all specimen surfaces was also performed. The objective of the present study is to investigate the in-beam fatigue behavior in the low oxygen potential atmosphere at 500 °C in order to contribute to the database of fusion reactor materials.

2. Experimental procedures

The material used in the present study was F82H steel (IEA heat). The chemical composition of F82H

* Corresponding author. Tel./fax: +81-298 59 2014.
E-mail address: murase.yoshiharu@nims.go.jp (Y. Murase).

0022-3115/$ - see front matter © 2004 Elsevier B.V. All rights reserved.
doi:10.1016/j.jnucmat.2004.04.021

steel is given in the previous paper [5]. Specimens with the geometry shown in Fig. 1 were punched from cold-rolled sheets with a thickness of 0.15 mm. The specimen size was $4 \times 10 \times 0.15$ mm in gauge, and a fatigue crack starter side-notch was spark erosion machined into the gauge from the edge to 0.60 mm in depth and 0.12 mm in width. Final heat treatments for the specimens were conducted at 940 °C for 30 min (normalizing) and at 750 °C for 60 min (tempering). These treatments yielded 100% tempered martensitic structure with average austenitic grain size of 19 μm diameter. Atomic displacement damage was introduced by 17 MeV protons with an incident beam flux of 2 $\mu A/cm^2$ during the in-beam tests. The damage rate was 1×10^{-7} dpa/s with an error of 10% in the specimen thickness of 150 μm. Circulating He gas flow in the irradiation chamber was adopted to control the specimen temperature. Although He gas was purified with a contamination absorber in the circulation system, a small amount of oxygen (10–3000 ppm) was detected in response to the degradation of the absorber during the experimental term between periodic maintenances. The partial pressure of oxygen was measured by the gas chromatography (Micro-GC, Varian-CP2000). An electrically heated He gas jet was used to reach the test temperature in both irradiation and unirradiation conditions. Chromel–alumel thermocouples were directly spot welded to the gauge to monitor the specimen temperature. The current to the electric heater for the He gas jet was controlled by the reference signal of the thermocouple in order to keep the specimen temperature at 500 °C. The temperature fluctuation was within 3 °C in the feedback system in both irradiation and unirradiated conditions. Details of the in-beam fatigue testing machine and specimen installation were described elsewhere [5,6]. The fatigue loading was triangular wave in tension–tension with the maximum stress of 227.9 MPa and the minimum stress of 100.3 MPa under a constant loading rate of 50 MPa/s. The maximum stress (σ_{max}) corresponded to 75% of the 500 °C yield stress at the notched ligament of the specimen. The minimum stress (σ_{min}) was arranged to give the loading ratio $R(\sigma_{min}/\sigma_{max}) = 0.44$.

Well-designed testing conditions as well as proper preparation of side-notched specimen played an important role in keeping the scattering of the number of cycle to fracture (N_f) within 10% in the present fatigue tests. After the fatigue tests, the fracture surfaces were examined by the scanning electron microscope (SEM, JEOL-5310). The observations of the specimen surfaces for all specimens were also conducted by means of the optical microscope (OM, OLYMPUS-BX60M).

3. Results

Fig. 2 presents the relative displacement in the gauge section of specimen at the maximum stress (227.9 MPa) with the number of cycles for the in-beam and unirradiation fatigue tests. The relative displacement is the difference of actual displacement at the maximum stress between the Nth cycle and the first cycle. As shown in Fig. 2, the number of cycles to fracture (N_f) was 12 390 and 13 491 for the in-beam tests, and the total dose level corresponded to 0.0064 and 0.0070 dpa, respectively. Fatigue life was slightly reduced under irradiation, namely, the average of N_f for the in-beam specimens corresponded to only about 80% of that for unirradiated specimens. After fatigue tests, the fracture surfaces were examined by SEM for all specimens. The fractographic appearance of the fracture surface was characterized by glide plane decohesions, quasi-cleavage facets and dimples for both in-beam and unirradiated specimens, with an indication of transgranular cracking in the mixed mode of ductile and brittle fractures. Striation-like patterns were detected on the fracture surface from the notch tip to the unstable fracture point for both specimens. In the present paper, the fatigue crack length (L_c) is designated as the distance from notch tip to the point

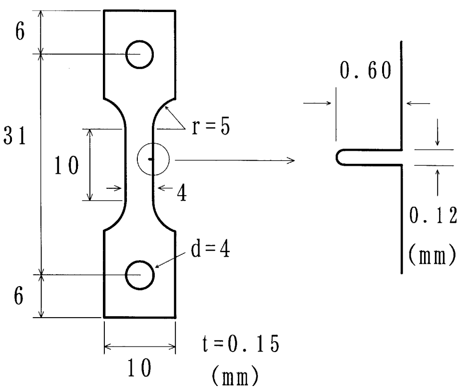

Fig. 1. Geometry of specimen for fatigue tests.

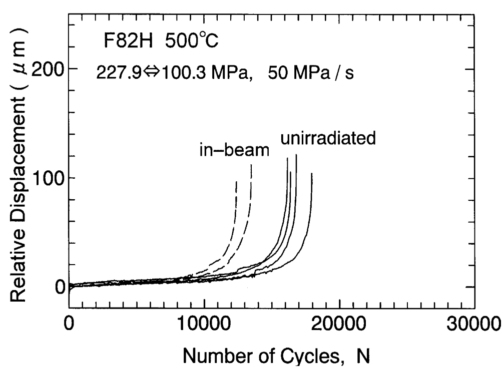

Fig. 2. Relative displacement of specimen in gauge section with number of cycles for in-beam and unirradiated fatigue tests.

where striation-like patterns disappear on the fracture surface. Fig. 3 shows SEM photos of the typical fracture surfaces observed from the angle of 45° to the loading direction for (a) in-beam and (b) unirradiated specimens. The enlarged photos of the fracture surfaces in the vicinity of the notch tip for each specimen are also presented in Fig. 3(a) and (b) with the respective descriptions of N_f and L_c. The fatigue crack length (L_c) was similar for both in-beam and unirradiated specimens. The formation of oxide film was observed on the fracture surface in the vicinity of the notch tip for the in-beam specimen (Fig. 3(a)), while it was not as clear as for the unirradiated specimen (Fig. 3(b)). Micro-cracks with preferential oxidation along them were formed on the specimen surface for both specimens, as shown in Fig. 3(a) and (b). The specimen surface was also examined by OM for all specimens. Fig. 4 shows OM photos and enlarged photos of the typical specimen surfaces for (a) in-beam and (b) unirradiated specimens. Oxidation was observed not only along the, grain boundaries but also on the crystallographic slip planes for both specimens. Especially in the in-beam specimen shown in Fig. 4(a), the oxidation appeared to be advanced enough to form numerous oxidation pits on the specimen surface.

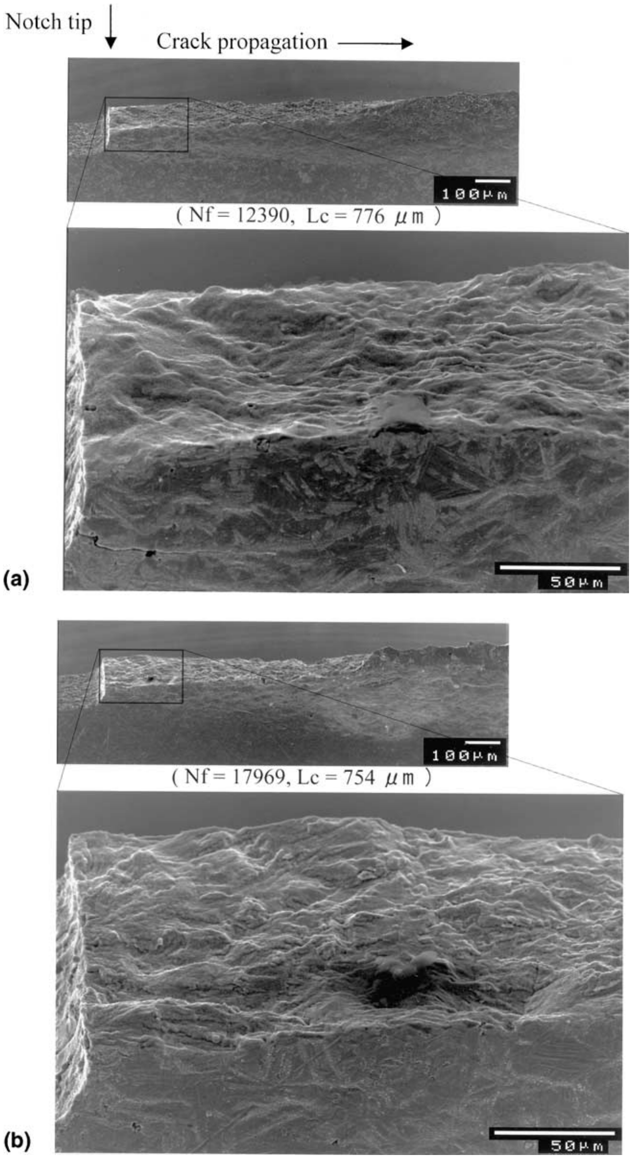

Fig. 3. SEM photos of typical fracture surfaces observed from the angle of 45° to the loading direction for (a) in-beam and (b) unirradiated specimens.

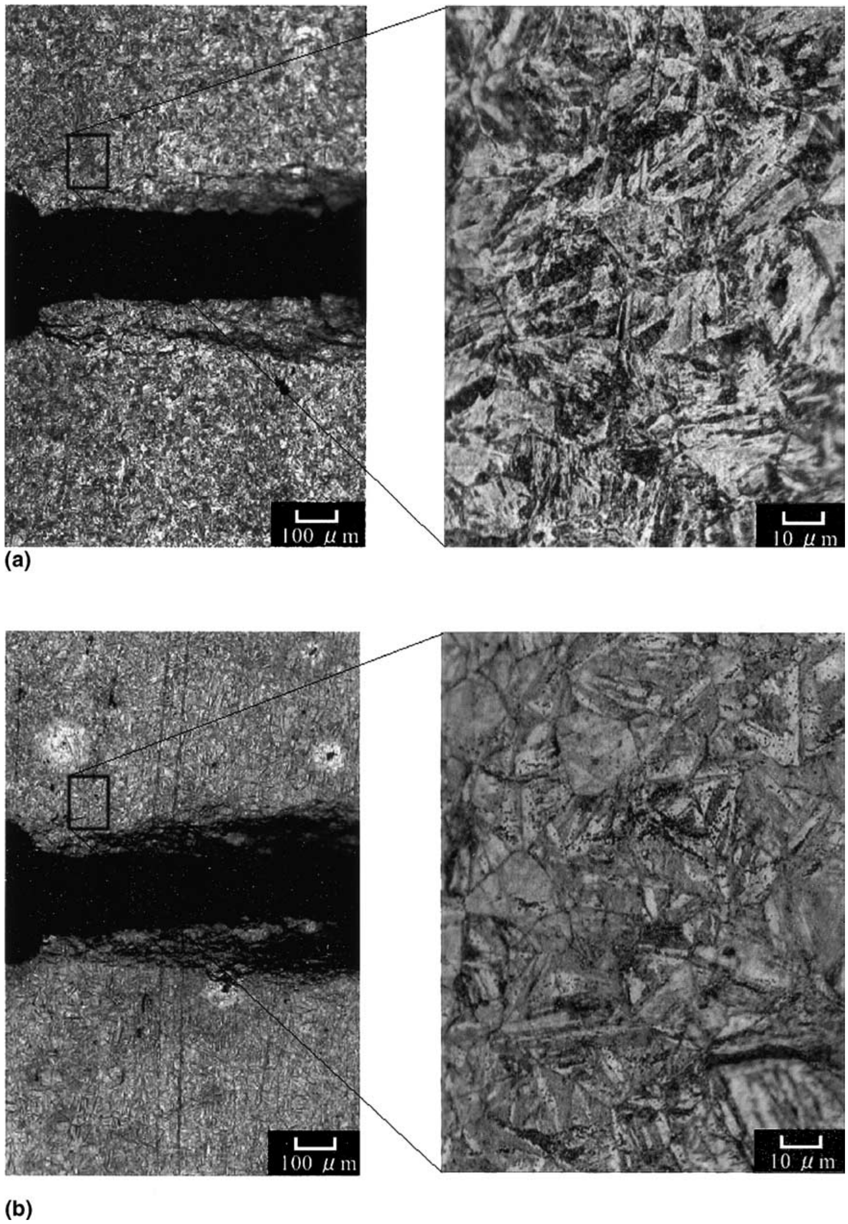

Fig. 4. Optical microscopy photos of typical specimen surfaces for (a) in-beam and (b) unirradiated specimens.

4. Discussion

In the previous work [5], a series of fatigue tests have also been conducted in an impure He atmosphere containing a small amount of oxygen (10–3000 ppm) at 60 °C. Since the oxidation could not be observed by SEM measurements on the surfaces of both in-beam and unirradiated specimens, it was assumed that the LT-type dynamic irradiation effect would be little influenced in such a low oxygen potential condition at 60 °C. However at higher temperatures, it is well known that some alloying elements are selectively oxidized to form an oxide scale on the alloy surface even in the low oxygen potential atmosphere [7,8]. Shida et al. [7] have reported the formation of chromium oxide scales on the surface of Alloy 800 in the impure He atmosphere of the simulated HTGR (high temperature gas-cooled reactors) environment at temperatures ranging from 700 to 850 °C. They have also pointed out that the intergranular oxidation could be attributed to the depletion of Cr resulting from the selective removal of Cr from the matrix into the external scale [7]. The injection and diffusion of Kirkendall vacancies followed by selective removal of Cr would play an important role in not only producing voids at various interfaces but also providing easy diffusion paths for oxygen from the surface to form oxides at the grain boundaries [7]. The interaction between oxidation and plastic deformation during cyclic loading has been indicated for various alloys tested in air at higher temperatures [9–12]. Parks et al. [9] have reported oxidation along the crystallographic slip bands on the surface of 9Cr–1Mo steels fatigued in air at 600 °C. Oxide scales initially formed on the surface could penetrate into the specimen interior under the processes of intrusion and extrusion at the slip bands during cyclic loading [9]. The surface oxide attack at former austenitic grain boundaries has also been discussed for 12Cr–Mo–V steel tested during cyclic loading in air at 600 °C [10]. The mechanism of oxidation along the grain boundaries during cyclic loading can be explained in terms of the preferential oxidation of newly created fresh surface due to the grain boundary sliding [10].

In the present study, oxidation was observed along the grain boundaries as well as on the crystallographic slip planes on the specimen surfaces of both in-beam and unirradiated specimens (see Fig. 4). This localized oxidation would be responsible for the interaction between oxidation and plastic deformation during cyclic loading. The formation of numerous oxidation pits on the surface of the in-beam specimen shown in Fig. 4(a) indicates the enhanced oxidation under irradiation and consequently the synergistic effects of oxidation and dynamic irradiation. Since the oxidation pit on the surface can act as a crack initiation point, the enhanced oxidation may promote crack initiation and lead to the reduction of N_f under irradiation (see Fig. 2). The formation of oxide films in the vicinity of notch tip on the fracture surface of the in-beam specimen, as shown in Fig. 3(a), also supports the enhanced oxidation under irradiation in the early stage of crack propagation. However, from the results of fractographic analysis on the fracture surface, the transgranular cracking mode with similar L_c was detected for both in-beam and unirradiated specimens (see Fig. 3(a) and (b)). The intergranular cracking induced by oxidation along the grain boundaries appears to be suppressed, probably because the relative higher amplitude of cyclic stress is imposed on specimens in the present fatigue loading condition. Therefore, the influence of the enhanced oxidation on crack propagation would be less significant than that of crack initiation.

In terms of the LT-type dynamic irradiation effect, less significant interaction of RID clusters with dislocations would be expected at higher temperatures such as 500 °C where the increase in defects recombination rate leads to the decrease in density of RID clusters. A slight decrease of N_f under irradiation at 500 °C shown in Fig. 2 may reflect not only the enhanced oxidation but also the reduction of LT-type dynamic irradiation effect. In the next study of the in-beam fatigue behavior in impure He atmosphere at higher temperatures, an extensive analysis of chemical components on the surface is definitely needed to clarify the synergistic effects of oxidation and dynamic irradiation.

5. Conclusions

From the experimental results, the following conclusions (1)–(3) can be drawn:

(1) Oxidation was observed along the grain boundaries as well as on the crystallographic slip planes on the specimen surfaces of both in-beam and unirradiated specimens. The localized oxidation would result from the combined effects of selective oxidation of Cr in the low oxygen potential atmosphere and the interaction between oxidation and cyclic loading.
(2) The formation of numerous oxidation pits on the surface of the in-beam specimens strongly indicates the enhanced oxidation under irradiation and consequently the synergistic effects of oxidation and dynamic irradiation. Since the oxidation pits on the surface can act as crack initiation points, the enhanced oxidation may promote crack initiation and lead to the reduction of fatigue life under irradiation.
(3) A slight decrease of fatigue life under irradiation at 500 °C may reflect not only the enhanced oxidation but also the reduction of the lower temperature type dynamic irradiation effect.

Acknowledgements

This work was financially supported by the Budget for Nuclear Research of the Ministry of Education, Culture, Sports, Science and Technology, based on the screening and counseling by the Atomic Energy Commission.

References

[1] P. Fenici, S. Suolong, J. Nucl. Mater. 191–194 (1992) 1408.
[2] R. Scholz, A.M. Morrissey, G. Bergamo, Radiat. Eff. Defect in Solid 129 (1994) 229.
[3] P. Marmy, J. Nucl. Mater. 212–215 (1994) 599.
[4] K. Sonnerberg, H. Ullmaier, J. Nucl. Mater. 103&104 (1981) 859.
[5] Y. Murase, J. Nagakawa, N. Yamamoto, ASTM STP 1418 (2002) 211.

[6] Y. Murase, J. Nagakawa, N. Yamamoto, Y. Fukuzawa, ASTM STP 1366 (2000) 713.
[7] Y. Shida, T. Moroishi, Corros. Sci. 33 (1992) 211.
[8] H.-P. Meurer, G.K. Gnirss, W. Mergler, G. Raule, H. Schuster, G. Ullrich, Nucl. Technol. 66 (1984) 315.
[9] J.S. Park, S.J. Kirn, C.S. Lee, Mat. Sci. Technol. A 298 (2001) 127.
[10] J.C. Earthman, G. Eggeler, B. Ilschner, Mat. Sci. Technol. A 110 (1989) 103.
[11] S. Nishio, W. Sakai, K. Yamada, Fatigue Frac. Eng. Mater. Struct. 19 (5) (1996) 581.
[12] R.L. Hecht, J.R. Weertman, Metall. Trans. A 24 (1993) 327.